

Intergranular properties of uniaxially pressed $\text{YBa}_2\text{Cu}_3\text{O}_{7-\delta}$ ceramic samples

I. García-Fornaris^a, E. Govea-Alcaide^{b,c,*}, P. Muné^c, and R.F. Jardim^b

^aDepartamento de Ciencias Básicas, Universidad de Granma,
Apdo. 21, P.O. Box 85100, Bayamo, Cuba.

^bInstituto de Física, Universidade de São Paulo,
C.P. 66318, 05315-970, S. Paulo, SP, Brazil.

^cDepartamento de Física, Universidad de Oriente,
Patricio Lumumba s/n, P.O. Box. 90500, Santiago de Cuba, Cuba,
*e-mail: malvarez@udg.co.cu

Recibido el 27 de julio de 2009; aceptado el 11 de enero de 2010

We performed measurements of electrical resistivity as a function of temperature, $\rho(T)$, in polycrystalline samples of $\text{YBa}_2\text{Cu}_3\text{O}_{7-\delta}$ (Y-123) subjected to different uniaxial compacting pressures. We observed by using X-ray diffractometry that samples have a very similar composition. Most of the identified peaks are related to the superconducting Y-123 phase. Also, from the X-ray diffraction patterns performed, in powder and pellet samples, we estimated the Lotgering factor along the $(00l)$ direction, $F_{(00l)}$. The results indicate that $F_{(00l)}$ increases from 0.13 to 0.16. From electrical resistivity measurements as a function of temperature, we were able to separate contributions arising from both the grain misalignment and microstructural defects. We found appreciable degradation in the normal-state transport properties of samples with an increase in uniaxial compacting pressure. It seems that this type of behavior is associated with an increase in the influence of microstructural defects at the intergranular level. The experimental results are analyzed in the framework of a current conduction model of granular samples.

Keywords: Bi-based cuprates; granular superconductors; electrical properties.

Se presentan mediciones de resistividad eléctrica como función de la temperatura en muestras policristalinas de $\text{YBa}_2\text{Cu}_3\text{O}_{7-\delta}$ (Y-123) sometidas a diferentes presiones de compactación antes de la sinterización final. Mediante el análisis de difracción de rayos-X se observó que las muestras poseen una composición muy parecida. En todos los casos la fase mayoritaria es de Y-123. Además, de los patrones de rayos X medidos en polvos y en pastillas, pudimos estimar el factor de Lotgering en la dirección $(00l)$, $F_{(00l)}$. Los resultados obtenidos indican que $F_{(00l)}$ aumenta ligeramente desde 0.13 hasta 0.16. De las mediciones de resistividad eléctrica como función de la temperatura separamos las contribuciones asociadas con la desorientación de los granos y los defectos microestructurales. Se encontró un deterioro de las propiedades eléctricas de las muestras en estado normal con el aumento de la presión de compactación. Los resultados sugieren que el comportamiento obtenido está asociado a un incremento de defectos microestructurales a nivel intergranular. Los resultados experimentales son analizados en el marco de un modelo de conducción eléctrica en estado normal propuesto para materiales granulares.

Descriptores: Cupratos basados en Bismuto; superconductores granulares; propiedades eléctricas.

PACS: 74.72.Hs; 74.81.Bd; 74.25.Fy

1. Introduction

In polycrystalline high- T_c superconductors the transport properties are mostly determined by its granular nature. The presence of current-path frustration such as voids, cracks, and grain boundaries in these samples is an unavoidable fact due to the preparation process, which results in ceramic materials. Grain boundaries play an important role in limiting the transport properties of polycrystalline superconductors. Moreover, it is well established that the properties of the grain boundaries control most of the macroscopic superconducting properties of all high- T_c materials [1]. It is believed that this phenomenon is mainly due to the misorientation between grains. [2] High angle grain boundaries act as Josephson coupled weak-links, leading to a significant field-dependent suppression of the supercurrent across the boundary [1]. A way to improve the transport properties of these materials is to subject them to large mechanical deformations. This technique has proven to be effective in raising the superconducting critical current, J_c , of the $\text{Bi}_{1.65}\text{Pb}_{0.35}\text{Sr}_2\text{Ca}_2\text{Cu}_3\text{O}_{10+\delta}$

superconducting tapes and ceramic samples, mainly due to a marked increase in the texture degree of a given sample. [2–6] Similar studies in $\text{YBa}_2\text{Cu}_3\text{O}_{7-\delta}$ are not extremely common. In this work we focus on the temperature dependence of electrical resistivity, $\rho(T)$, of $\text{YBa}_2\text{Cu}_3\text{O}_{7-\delta}$ samples subjected to different uniaxial compacting pressures before the last heat treatment. X-ray diffraction (XRD) analysis has been performed as complementary characterization. The main contribution of this paper is in studying the influence of the uniaxial compacting pressure on the intergranular transport properties of Y-123 samples.

2. Experimental procedure

Polycrystalline samples of $\text{YBa}_2\text{Cu}_3\text{O}_{7-\delta}$ (Y-123) were prepared from powders of Y_2O_3 , BaCO_3 , and CuO , which were mixed in an atomic ratio of Y:Ba:Cu (1:2:3). The mixture was first calcined in air at 900°C for 24 h. Then, the powder was reground and pressed into pellets 15 mm in diameter and

0.5 mm thick at different compacting pressures ranging from 190 to 250 MPa. These pellets were heat treated at 950°C for 24 hrs. in air. The last heat treatment was performed in oxygen at 700 °C for 30 hrs. followed by slow cooling.

We have evaluated the phase identification in both powder and bulk samples by means of X-ray diffraction patterns obtained in a Bruker-AXS D8 Advance diffractometer. These measurements were performed at room temperature using Cu K α radiation in the $3^\circ \leq 2\theta \leq 80^\circ$ range with a 0.05° (2θ) step size and 5 sec counting time.

The temperature dependence of the electrical resistivity, $\rho(T)$, was measured by using the standard dc four-probe technique. Before each measurement, the samples were cooled from room temperature down to 77 K. Then, the excitation current that was injected along the major length of samples. Both the voltage across the sample and its temperature were collected while the temperature was raised slowly to 300 K. The typical dimensions of samples are $t = 1$ mm (thickness), $w = 2$ mm (width), and $l = 10$ mm (length). Also, the excitation current in our measurements was 1 mA.

3. Results and discussion

Figure 1 displays the X-ray diffraction patterns taken on bulk samples **Y1**, and **Y2**. The results shown in this figure indicate that both samples have similar chemical composition. Also, the identified indexed reflections are related to the Y-123 ($\text{YBa}_2\text{Cu}_3\text{O}_{7-\delta}$) phase. The unit-cell parameters were calculated with respect to an orthorhombic unit cell and the obtained values $a = 3.872$ Å, $b = 3.826$ Å, and $c = 11.751$ Å are similar to those reported elsewhere for the underdoped $\text{YBa}_2\text{Cu}_3\text{O}_{6.56}$ material [5]. In order to evaluate the orientation degree of the $(00l)$ planes in samples subjected to different uniaxial compacting pressures, we calculated the Lotgering factor, $F_{(00l)}$, by using the expression [6, 7]:

$$F_{(00l)} = \frac{P - P_0}{1 - P_0}, \quad (1)$$

where $P_0 = I_{0(00l)} / \sum I_{0(hkl)}$ and $P = I_{(00l)} / \sum I_{(hkl)}$. Here, $I_{0(00l)}$ and $I_{0(hkl)}$ are the intensities of the $(00l)$ and (hkl) peaks for a powder sample, respectively. On the other hand, $I_{(00l)}$ and $I_{(hkl)}$ are the intensities of the $(00l)$ and (hkl) peaks, respectively, for a pellet sample. Values of $F_{(00l)}$ are in range from 0 (non-oriented samples) to 1 (highly oriented samples). The obtained values for samples **Y1** and **Y2** are 0.13 and 0.16, respectively. These results suggest that the uniaxial compacting pressure are not enough to produce appreciable changes in the grain orientation of the samples, at least within the range of 190 - 250 MPa.

All samples were also characterized by measurements of electrical resistivity versus temperature. Figure 2 shows the $\rho(T)$ curves for samples **Y1** and **Y2**. The most important features of these can be summarized as follows:

- (a) both curves start to deviate from the linear behavior at high temperatures below the onset temperature $T_{on} \sim 96$ K,

- (b) electrical resistivity at $T = 270$ K increases $\sim 80\%$ between 1.72 mΩ cm, in **Y1**, and 9.86 mΩ cm, in **Y2**,
- (c) the temperature in which the zero resistance state is observed, T_{off} decrease from 83 K in the sample **Y1** to 80 K in **Y2**.

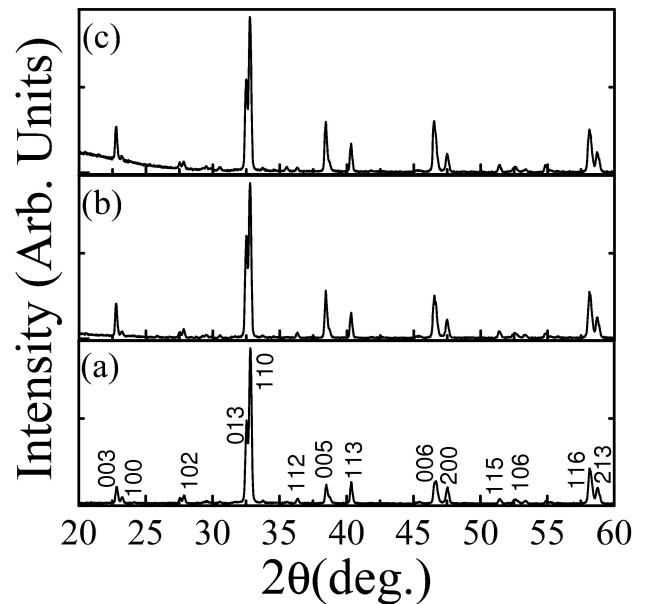


FIGURE 1. X-ray diffraction patterns of a powder sample (a), and bulk samples **Y1** (b), and **Y2** (c). The reflections belonging to the Y-123 phase are marked by Miller indexes in (a).

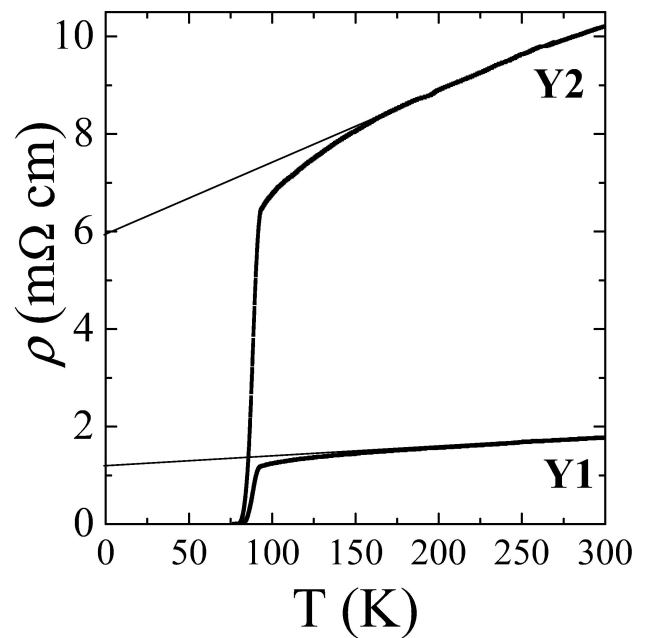


FIGURE 2. Temperature dependence of the electrical resistivity of samples **Y1** and **Y2**. Some physical parameters of samples, extracted from linear fitting of $\rho(T)$ curves, are displayed in Table I (see comments in the text).

TABLE I. Relevant parameters extracted from the analysis of the electrical resistivity as a function of temperature, $\rho(T)$: the linear slope of $\rho(T)$, A , the residual resistivity at $T = 0$, $\rho(0)$, the effective area factor, α_n , and the intergranular electrical resistivity, ρ_{wl} .

Sample	A ($\mu\Omega \text{ cm/K}$)	$\rho(0)$ ($\text{m}\Omega \text{ cm}$)	α_n	ρ_{wl} ($\text{m}\Omega \text{ cm}$)
Y1	2.24	1.12	0.18	0.20
Y2	14.11	6.09	0.04	0.24

Notice that the onset temperature is related to the transition of the isolated grains to the superconducting state and its constant value in both samples strongly suggests that the grains have similar stoichiometry. This result is in excellent agreement with those of XRD and the magnetometric measurements.

On the other hand, T_{off} is related to:

- (1) the volume fraction of the Y-123 phase,
- (2) the features of the intergranular component and/or
- (3) the oxygen content.

Thus, as the chemical composition of grains is similar then the observed behavior of the offset temperature may be related to changes in the last two points with an increase in uniaxial compacting pressure [8]. The above results suggest a deterioration in both the normal and the superconducting transport properties of Y-123 samples with an increase in uniaxial compacting pressure.

In order to quantify the evolution of the microstructure with increasing compacting pressure and its effect on the transport properties, we analyze the temperature dependent electrical resistivity $\rho(T)$ data, in the normal-state region ($T > T_{on}$), by using the current conduction model proposed by Díaz *et al.* [8]. In such a model, the electrical resistivity data is described by the equation:

$$\rho(T) = \frac{1}{\alpha_n} (\rho_{ab}(T) + \rho_{wl}), \quad (2)$$

where α_n is given by

$$\alpha_n = f \alpha_{str}, \quad (3)$$

and is an effective area factor that represents the contributions of both misalignment of the grains (texture degree) f ($0 < f \leq 1$) and microstructural defects such as voids and microcracks α_{str} ($0 < \alpha_{str} \leq 1$). Also, in this model the grains are believed to behave as a single crystal, so that the first term in Eq. (2), ρ_{ab} , is related to the average of the electrical resistivity in the ab-plane. This term in our analysis has been assumed to be linearly temperature dependent with slopes $A_{sc} = 0.5 \mu\Omega \text{ cm/K}$ [8]. In addition, we assumed the zero-residual temperature intercept as obtained from the data of single crystals materials [8]. The term ρ_{wl} , in Eq. (2), is the average intergranular electrical resistivity that is assumed

to be temperature-independent. Additionally, both α_n and ρ_{wl} can be obtained by utilizing the expressions [8]:

$$\alpha_n = \frac{A_{sc}}{A}, \quad (4)$$

and

$$\rho_{wl} = \alpha_n \rho(0), \quad (5)$$

where A is the slope of the $\rho(T)$ curve in the T-linear region, and $\rho(0)$ the residual resistivity at $T = 0$ (see Table I). Both parameters were obtained by fitting the $\rho(T)$ data to the typical linear dependence $\rho(T) = AT + \rho(0)$. We want to point out that in our experimental conditions the estimation of parameters α_n and ρ_{wl} have a relative error of 10%.

By using Eqs. (4) and (5) in combination with values of A_{sc} , A , and $\rho(0)$, we were able to obtain the values of α_n and the average intergranular electrical resistivity (see Table I). The analysis of values of the parameter α_n , for Y-123 samples, shows appreciable decrease with an increase in uniaxial compacting pressures. Within the framework of the current conduction model proposed by Díaz *et al.*, *i.e.* see Eq. (3), the above-mentioned result is related to a decrease in the texture degree of samples and an increase in the microstructural defects. As indicated by the estimation of the Lotgering factor, the textured degree of Y-123 samples slightly increases in the sample **Y2**. Thus, the observed decrease of α_n can be associated with the influence of microstructural defects. It seems that increasing the uniaxial compacting pressure in these samples favors the appearance of cracks and/or impurities as also indicated by the increase of 17 % in the intergranular electrical resistivity, ρ_{wl} .

In order to get more information about this, let us estimate the values of the microstructural factor α_{str} . As suggested, the definition of α_n ($= f \alpha_{str}$) we need values of the grains misalignment factor, f . Díaz *et al.* reported values of $f \approx 0.33$ that were obtained by using a model derived from the application of the Effective Medium Approximation [8]. This value indicates that the Y-123 is a nontextured sample, in good agreement with the low values of the Lotgering factor obtained in this work. Our results also indicate that increasing the uniaxial compacting pressure does not result in appreciable changes in the texture degree of samples. Hence, if we assume that $f = 0.33$, then α_{str} is 0.55 and 0.12 for samples **Y1** and **Y2**, respectively. Notice that in this case, the obtained results ensure an increase in microstructural defects in samples with an increase in uniaxial compacting pressure.

4. Conclusions

We have studied in detail the influence of the uniaxial compacting pressure on the granular structure of both $\text{YBa}_2\text{Cu}_3\text{Cu}_{7-\delta}$ (Y-123) samples by means of transport measurements. X-ray diffraction patterns, magnetic and transport measurements confirm that the samples exhibit similar intragrain properties. By using a current conduction model we were able to separate the influence of factors such as the

grain alignment and microstructural defects from the $\rho(T)$ data. In this case, the results indicate a worsening in the transport properties with an increase in uniaxial compacting pressures. Moreover, the above-mentioned behavior is mostly associated with the influence of microstructural defects such as cracks. The observed results in these samples differ appreciably from those reported in $\text{Bi}_{1.65}\text{Pb}_{0.35}\text{Sr}_2\text{Ca}_2\text{Cu}_3\text{O}_{10+\delta}$ ceramics samples, thus ensuring better mechanical properties in this compound.

Acknowledgments

This work was supported by the Brazilian agencies Fundação de Amparo à Pesquisa do Estado de São Paulo (FAPESP) under Grant No. 05/53241-9 and Conselho Nacional de Desenvolvimento Científico e Tecnológico (CNPq) under Grant No. 473932/2007-5. One of us E.G-A. acknowledges FAPESP under Grant No. 2009/51562-3. R.F.J. is CNPq fellow under Grant No. 308706/2007-2.

-
1. H. Hilgenkamp and J. Mannhart, *Rev. Mod. Phys.* **74** (2002) 485.
 2. T.T. Tan *et al.*, *Supercond. Sci. Tech.* **14** (2001) 471.
 3. E. Govea-Alcaide, R.F. Jardim, and P. Muné, *Physica C* **423** (2005) 152.
 4. E. Govea-Alcaide, I. García-Fornaris, P. Muné, and R.F. Jardim, *Eur. Phys. J. B* **58** (2007) 373.
 5. W. Wong-Ng and L.P. Cook, *Adv. Ceram. Mater.* **2** (1987) 624.
 6. T. Kobayashi, R. Ogawa, K. Miyazawa, and M. Kuwabara, *J. Mater. Res.* **17** (2000) 79.
 7. S. A. Saleh, *Physica C* **444** (2006) 40.
 8. A. Díaz, J. Maza, and F. Vidal, *Phys. Rev. B* **55** (1997) 1209.